On hydrogen adsorption by nanodispersed MoS2-based catalysts

P. Afanasiev, H. Jobic

On the hydrogen adsorption by nanodispersed MoS_2 – based catalysts.

Pavel Afanasiev* and Herve Jobic

Univ Lyon, Université Claude Bernard Lyon 1, CNRS, IRCELYON, F-69626, Villeurbanne, France.

Abstract

The nature and the amount of hydrogen species adsorbed on MoS_2–based catalysts have been studied by inelastic neutron scattering (INS) as a function of preparation and treatment conditions. Unsupported MoS_2 materials have been prepared from $(NH_4)_2MoS_4$ in pure H_2S or in H_2 flow and optionally doped with Co, Ni and Pt. The results of INS were compared with other characterizations including temperature programmed reduction (TPR), temperature programmed desorption (TPD) and catalytic tests in thiophene hydrodesulfurization (HDS). The results of INS study suggest that major hydrogen species is of similar type, independently on the preparation conditions and promotion. The observed INS frequencies were compared with the results of DFT calculations carried out for different configurations of M- and S- edges of (doped) MoS_2 slabs. The main feature for all samples near 685-692 cm^{-1} corresponds to the vibrations of dangling –SH groups linked to six-coordinate Mo atoms, generated by hydrogenolysis of the S-S bonds at the M edges of MoS_2 slabs. A minor signal is present as a shoulder at 610-625 cm^{-1}, most pronounced in the Co promoted and sulfur-saturated solid, which is probably due to interaction of the SH groups with adjacent Co atoms and/or neighboring S_2^{2-} groups. The total amount of adsorbed H species depends on the treatment conditions, decreasing with the degree of material reduction.

Keywords: Inelastic neutron scattering; molybdenum sulfide; hydrogen adsorption; hydrodesulfurization catalysts

Introduction

Molybdenum disulfide (MoS_2) is a main component of $Co(Ni)MoS_2/Al_2O_3$ industrial hydrotreating (HDT) catalysts. The active phase of HDT catalysts contains nanoscopic slabs of MoS_2 decorated at the edges with Co or Ni [1]. Unsupported sulfides are widely studied as well, for the novel generation of highly active HDT catalysts [2, 3] or as

dispersed catalysts for upgrading heavy residuals [4]. Beyond HDT, MoS_2 shows interesting performance for alcohols synthesis [5, 6], carbon oxides hydrogenation [7, 8] or water gas shift [9]. In the recent years MoS_2 also attracted much attention as a promising material for electrochemical hydrogen evolution reaction (HER) [10, 11] or as a component of photocatalysts aimed at water splitting, where it is used as a hydrogen production co-catalyst [12, 13]. In all these applications hydrogen activation and/or associative desorption is involved.

Hydrogen adsorption on MoS_2 edges has a fundamental importance for the understanding of the whole catalytic act. Indeed, for any HDS reaction to occur, adsorption of an S-containing molecule and dissociative adsorption of H_2 are necessary. Similarly, for HER process, recombination of adsorbed H species is necessary. Determining the state of adsorbed hydrogen in the MoS_2-based catalysts would improve control of the surface species involved in the elementary steps.

Despite the importance of the topic, there are relatively few experimental works on the adsorption of hydrogen on MoS_2. Topsoe et al using infrared spectroscopy provided the first indirect evidence of the presence of -SH groups in the supported catalysts [14]. Inelastic neutron scattering (INS) is one of the few methods of straightforward spectroscopic observation of H species. Bulk MoS_2 prepared by decomposition of $(NH_4)_2MoS_4$ in 10% H_2S/H_2 at 400 °C was studied by Jones et at in the range of pressures 1-50 bar [15]. Only S-H bending at 82 meV (660 cm^{-1}) was observed beside lattice vibrations and molecular hydrogen. Bulk and supported MoS_2 has been studied by INS Wright et al [16, 17, 18] for the MoS_2 samples prepared by reduction of MoS_3 in flowing hydrogen at 400°C. Vibration at 650-670 cm^{-1} was observed and it has been concluded that hydrogen is bonded to one or more sulfur atoms rather than to metal atoms. Later, H_2 sorption at pressures from 1 to 30 bar was studied by INS by Sundberg et al [19], and Mitchell et al [20]. Pure and Ni- promoted MoS_2 and alumina - supported MoS_2 were treated at 673 K in 10%H_2S/H_2 (and re-sulfided at 573 K) were studied in [19]. Again, on bulk MoS_2 a bending S-H vibration at 650-670 cm^{-1} has been observed. The stretching frequency appeared at 2500 cm^{-1}. To maximize the amount of adsorbed H_2, MoS_2 was treated in hydrogen at 1200 K in Ref. [20], which in fact leads to a drastic drop of the H_2 uptake [21]. In the previous studies no structural attribution had been provided

relating the observed species to the existing models of MoS_2 slabs, which predict the existence of structurally distinct slabs edges, so called S-edge and M-edge [22]. The influence of treatment conditions and/or that of the presence of a second metal on the H_2 adsorption by unsupported MoS_2 was never accessed by INS.

Many theory works have been published on the H_2 activation by MoS_2. Some earlier works dealt with heavily reduced MoS_2, supposing heterolytic dissociation to Mo-H on sulfur vacancies and adjacent S-H species [23]. On the other hand, Byskov et al suggested that homolytic activation is favored for CoMoS catalysts leading to formation of -SH groups on the S-edge [24, 25]. Cristol et al carried out DFT calculations of the H_2 adsorption on the [100] MoS_2 surfaces for various edge stoichiometries. A thermodynamic diagram was built, relating the edges stoichiometry to the nature of adsorbed hydrogen atoms, as a function of the total pressure and of the P_{H2S}/P_{H2} ratio. The S−H groups were identified as stable adsorption form of hydrogen [26]. Travert et al studied activation of hydrogen on MoS_2 edges and found that migration of adsorbed hydrogen from Mo atom to an S atom is almost athermic, leaving the possibility for existence of both Mo-H and –SH stable species [27]. Sun et al concluded that on the unpromoted MoS_2 and on the Co-promoted S-edge, H_2 adsorption generates stable surface -SH groups. Addition of Co was predicted to increase the amount of adsorbed H_2, whereas promotion with Ni - to decrease it [28, 29]. Lauritsen et al combining scanning tunneling microscopy (STM) of single-layer MoS_2 nanoclusters with DFT concluded that on the hexagonal MoS_2 flakes, S-edges contain adsorbed S-H groups [30]. Dinter et al studied 100 %S-covered M-edge and found that the rate-determining step for the onset of reduction is dissociative chemisorption of H_2 on two adjacent S_2 dimers on the M-edges [31]. Later, Prodhomme calculated S-H vibration frequencies partially sulfur-covered M- and S-edged and found the values close to the experimental values of 2500 cm^{-1} for stretching and 650 cm^{-1} for bending on both M- and S-edges [32].

Each of these theory works is supported by a subset of INS and other experimental data, but no coherent picture emerges on the nature and the amount of stable adsorbed hydrogen species as a function of treatment conditions and the presence of promotor. Thus adsorption is concluded to be predominant on S-edge in [30] whereas no clear preference was given to M- or S- edge in [32].

This work reports on the INS study of a series of samples differing by the MoS_2 reduction and/or the presence of a second metal. We inquire how these parameters influence the amount and the nature of stable adsorbed hydrogen species. DFT calculations of the vibration frequencies have been carried out to explain the experimental results.

2. Experimental

2.1. Materials preparation

All chemicals were high purity products purchased from Sigma-Aldrich. Ammonium thiomonomolybdate $(NH_4)_2MoS_4$ was obtained by adding 15 g of $(NH_4)_6Mo_7O_{24}\cdot 4H_2O$ to 200 mL of a 20 wt % solution of $(NH_4)_2S$ at ambient temperature. The precipitated red crystals were thoroughly washed with small amounts of ethanol and tetrahydrofuran (THF), dried and stored under nitrogen.

Decomposition of ATM was carried out in Pyrex or quartz reactors. A weighted amount of ATM was placed in a reactor and treated in a gas flow of 10 L/h of pure H_2 or pure H_2S. The temperature was raised at a rate 5° min^{-1} to a desired value and kept for 2 h.

Promoted catalysts were prepared according to Ref. [33]. In brief, a weighted amount of Ni(II) or Co(II) acetylacetonate was dissolved in a minimum amount of methanol while flushed by nitrogen. Then MoS_2 powder was added to the solution in an atomic ratio of Co(Ni)/Mo = 0.4 and then the suspension was heated at the boiling temperature of methanol (65 °C) for 4 h without air admission. Then the mixtures were cooled to room temperature and kept overnight under nitrogen. Afterward, the solids were recovered by filtration and dried under N_2 at room temperature. The catalysts were tested after re-sulfidation with H_2/H_2S at 350 °C for 1 h. Platinum – containing material was prepared by means of impregnation of MoS_2 (prepared in H_2 at 400 °C) with aqueous tetraammineplatinum (II) nitrate solution, followed by re-sulfidation in 15% vol. H_2S/H_2 for 2h and then by treatment in hydrogen flow at 400°C for another 2h.

To carry out hydrogen adsorption, for all preparations under study, the samples were cooled down to room temperature under the same gas atmosphere as was used for activation (H_2S, H_2, or their mixture), then the gas flow was changed to pure H_2 flow at 10 L/h and kept for 2h. Then, in order to remove physically adsorbed hydrogen-containing species, the sample was flushed in 10 L/h nitrogen flow for 1 h at room

temperature. It was then placed into a sealed stainless steel container for INS experiment, without delay.

2.2. Characterizations

Transmission electron microscopy (TEM) was carried out on a JEOL 2010 device with an accelerating voltage 200 keV. The samples were dispersed in *n*-hexane by ultrasound, and then put onto a holey carbon filament on a copper grid sample holder. The analysis of images was carried out using Digital Micrograph Gatan™ software. Nitrogen adsorption was carried out on a Micromeritics ASAP 2010 instrument and calculated using BET equation. Prior to measurements the samples were heated in a secondary vacuum at 300 °C for 4 h. The X-ray diffraction (XRD) patterns were obtained on a Bruker diffractometer with Cu Kα emission and crystalline phases were identified using standard JCPDS files. Temperature-programmed reduction (TPR) was carried out in a quartz reactor. The samples of sulfides (ca. 0.01 g) were linearly heated under a hydrogen flow (50 cm^3 min^{-1}) from room temperature to 1050 °C (heating rate 5° /min). Hydrogen sulfide and other gases evolved upon reduction were detected by means of Thermo Fischer quadrupole mass-spectrometer. Temperature programmed desorption (TPD) in argon flow was carried out in the same setup as used for TPR, but the sample mass was increased to 0.2 g in order to improve the signal to noise ratio. The amounts of H_2S and H_2 released from the solids were quantified after calibration of the MS with gas mixtures of known H_2S and H_2 content, containing respectively 500 ppm H_2S and 1 % vol. of H_2 in Ar. X-ray photoelectron spectroscopy (XPS) was carried out on a VG ESCALAB 200R device using Al Kα radiation. The binding energies (BE) were referred to the energy of the C 1s peak (BE 285.0 eV). Quantification of the surface contents was done using the sensitivity factors provided with the VG software. Metals content was analyzed after dissolution in a HNO_3/H_2SO_4 mixture, by plasma-coupled atomic emission spectroscopy (AES-ICP). Analysis of light elements (CHNSO) was carried out on a Thermo Fisher Flash 2000 device.

2.3. Inelastic neutron scattering (INS)

Weighted amounts about 8 g of each material were prepared and transferred to the stainless steel containers for INS measurements, under inert atmosphere. INS experiments were performed on the IN1BeF spectrometer, at the Institut Laue-Langevin, Grenoble, France. The INS spectra were measured from 240 to 2800 cm^{-1}. A beryllium filter was placed between the sample and the detector. This setting gives a moderate energy resolution, with an instrumental resolution varying from 25 cm^{-1} at small energy transfers to 50 cm^{-1} at large energy transfers. The frequency values were corrected from a systematic shift due to the beryllium filter. The estimated resolution is ~20 cm^{-1}. The spectra were recorded at 5 K to decrease the mean-square amplitude of the atoms and, thus, to sharpen the vibrational features.

2.4. Thiophene HDS test

Catalytic activity in thiophene hydrodesulfurization (HDS) reaction was measured at atmospheric pressure in a fixed-bed flow microreactor. Reaction was carried out in the temperature range 300–340 °C, under 50 mL/min gas flow, using 50–100 mg of catalyst and partial pressure of thiophene 2.7 kPa. The plug-flow reactor model was used to calculate the specific reaction rate, Vs, according to the equation $Vs = -(F/m)\ln(1 - x)$ where F is the thiophene molar flow (mol/s), m is the catalyst mass (g), and x is thiophene conversion. Catalytic activity was estimated at steady state conversion, after at least 16 h on-stream. Arrhenius plots were built using five temperature points between 300 and 340 °C. High correlation coefficient (better than 0.995) and physically reasonable activation energy between 17 and 22 Kcal/mol were used as criteria of successful activity measurement in the kinetic regime. In all experiments thiophene conversion was below 10 %, allowing to use pseudo-first order kinetics equation. For each catalyst at least two HDS tests have been carried out.

2.5. DFT calculations

Small MoS_2 clusters were simulated using ORCA code [34]. Triangular clusters were used, providing the maximal edge length vs. the total number of atoms. In the DFT calculations, generalized gradient PBE and BP86 functionals were used in combination with Ahlrichs family def2-SVP and def2-TZVP basis functions, under RIJCOSX approximation for Coulomb and HF Exchange. Considerable convergence problems have

been encountered, in particular for the open-shell configurations. To achieve convergence, a two-step scheme was applied. First, geometry optimization was carried out with def2-SVP basis and loose convergence criteria and then final calculation was carried out from the molecular orbitals and geometries of these intermediate optimized structures taken as input but using larger basis, fine grid, tight convergence tolerance and SlowConv or VerySlowConv options (high mixing degree). Examples of input files and optimized structures are available in the SI.

To select an appropriate model size, clusters with n= 3 to 7 (n is number of metal atoms on an edge) have been studied and the frequencies compared as a function of n. It appears that from n=4 onward the calculated frequencies weakly depend on the n. In order to reduce the computation cost without losing accuracy, n=5 clusters have been retained. Such clusters correspond to small MoS_2 flakes yet observable by conventional TEM (~1.3 nm size). All-electron calculations were implemented. All atoms were relaxed, which seems important for the frequency calculations, because (i) normal vibration modes involve movements of variable number of neighboring atoms sometimes extending relatively far; and (ii) unphysical results were often obtained on the constrained models. As calculation of analytical frequencies presented serious convergence problems, numeric frequencies were finally preferred, that are more stable though arguably less accurate. In cases when both types of frequency calculations converged, the difference of frequencies did not exceed several cm^{-1}

3. Results and discussion

In this work we focus on five MoS_2-based materials prepared by the same technique but differing by the conditions of preparation and by the presence of a second metal (Co, Ni Pt). The designations of materials are self-explanatory, indicating composition and activation conditions. One sample (MoS_2-H_2S-350) was prepared in pure H_2S at 350 °C; two (Co-MoS_2-H_2SH_2-350 and Ni-MoS_2-H_2SH_2-350) were activated in a H_2S/H_2 mixture at 350 °C and two others (MoS_2-H_2-400 and Pt-MoS_2-H_2-400) were prepared in pure H_2 at 400 °C. This choice of samples was a compromise between the goal to obtain maximum information and limited time available for the INS run. The solids as prepared are supposed to have different sulfur coverage of edges and different proportion of S- and

M-edges in the 2D MoS_2 slabs morphology. Thus, according to ab initio theory studies [35], a solid prepared in pure H_2S such as MoS_2-H_2S-350 should expose almost exclusively M-edges, whereas molybdenum sulfide samples obtained under hydrogen flow as (Pt)MoS_2-H_2-400 should expose comparable amounts of S– and M- edges.

3.1. Characterizations

The influence of preparation conditions on the catalytic and physical properties in a similar series of unsupported MoS_2 catalysts has been studied previously [21]. However a considerable scale up was necessary to comply with the requirements of INS experiment. Whereas the mass of prepared samples in [20] was in the range 0.5-1 g, here we prepared 8-9 g of each sample using the same lab equipment. We characterized the solids as prepared using a set of usually applied techniques (XRD, BET, XPS, TEM, chemical analysis). The main properties of the solids under study are summarized in the Table 1. The results of TEM, XRD and XPS characterizations are provided in the SI. According to XRD, all samples are dispersions of poorly crystalline 2H-MoS_2 (Fig. S1). In the bimetallic catalysts (Co, Ni, Pt)-MoS_2, no phases containing the second metal were observed. Analysis of the (002) XRD line width using Scherer formula gives the mean stacking from 3 to 5. In agreement with XRD, TEM shows bundles of MoS_2 slabs with 3-6 nm length and stacking from 2 to 7, typical for these preparations (Fig. S2). The specific surface area is in the range 51-64 m^2/g, in agreement with our previous studies of ATM- derived MoS_2 [21].

Chemical analysis (Table 1) shows that four of five samples are overstoichiometric with respect to sulfur, the highest excess of sulfur found in the MoS_2 prepared in pure H_2S. The most reduced Pt-doped sample is slightly understoichiometric. The amounts of Co and Ni after washing and re-sulfidation are far below the initial atomic ratio M/Mo = 0.4 (M = Co, Ni), showing that only a part of Ni or Co introduced in the reflux mixtures was grafted at the edges, whereas the excess of Ni(Co) acetylacetonate remained in the solution. Grafting of nickel appears less efficient than for cobalt. The amount of Pt (introduced not by grafting but by impregnation), was fixed at the 3% wt. level (Table S1). Accessing the H content by chemical analysis is difficult as it gives poorly reproducible results. Indeed, recently we demonstrated that edge -SH groups in freshly

prepared bulk MoS_2 are labile in air and totally disappear during the first hour of air exposure, being replaced by hydroxide groups and water. Moreover, continuous increase of the amount of OH groups occurs in time, due to air humidity [36]. By this reason chemical analysis (CHONS), even after a short air exposure, seems less reliable as a method of H species quantification than the temperature programmed desorption (TPD) technique as discussed in the following sections.

Table 1 Properties of the sulfide materials under study

Sample	S_{BET} m^2/g	XRD size (nm)	L/S [a]	TOF_{HDS} [b]	Chemical Composition	INS H uptake x [c]
MoS_2-H_2S-350	64(5)	3.4(5)	5/4±1	7.7(6)	$H_{0.057}MoS_{2.37}$	0.057(3)
MoS_2-H_2-400	55(5)	3.7(5)	6/5±1	4.2(4)	$H_{0.044}MoS_{2.03}$	0.041(3)
Co-MoS_2-H_2SH_2-350	53(5)	3.5(5)	5/4±1	37(3)	$H_{0.039}Co_{0.054}MoS_{2.11}$	0.045(3)
Ni-MoS_2-H_2SH_2-350	57(5)	3.6(5)	5/4±1	17(2)	$H_{0.044}Ni_{0.037}MoS_{2.13}$	0.046(3)
Pt-MoS_2-H_2-400	51(5)	3.9(5)	6/5±1	12(1)	$H_{0.024}Pt_{0.023}MoS_{1.99}$	0.028(2)

[a] L – mean length (nm), S- stacking; indicated measurement error is the same for both values; [b] TOF, h^{-1} approximately calculated with respect to BET surface area and part of exposed edges as observed by TEM; [c] the values for x in the chemical formulae ($H_xMoS_{2+\delta}$) obtained by integration of the main INS peak and normalized with respect to the first sample, in which the same value as measured by TPD is assumed.

XPS shows full sulfidation of the samples (Fig. S3, Table S1). Low amounts of Mo(VI) and S(VI) surface impurities come probably from the imperfections of the sample transfer system. Transition metals are all mostly in the sulfide state, except of platinum, which after reduction at 400 °C in H_2 is present in the state closer to metal (Table S2). The signal to noise ratios in the spectra of the dopant metals were not sufficient to make reliable decomposition for fine analysis of species, e.g. to unravel between Co(Ni)MoS decorated sites and individual (Co, Ni) sulfides, but Co $p_{3/2}$ signal maximum at BE 778.4 eV is close to that reported for the CoMoS phase [37]. According to XPS, the dispersion of Co seems to be better than that of Ni and Pt (Table S2). Significant difference was observed between the composition of sulfur species in the MoS_2-H_2S-350 sample that contains 24 % of S(-I) and reduced sample MoS_2-H_2-400 and Pt-MoS_2-H_2-400 in which the amount of S(-I) from disulfide groups is considerably lower (Figure S4, Table S1).

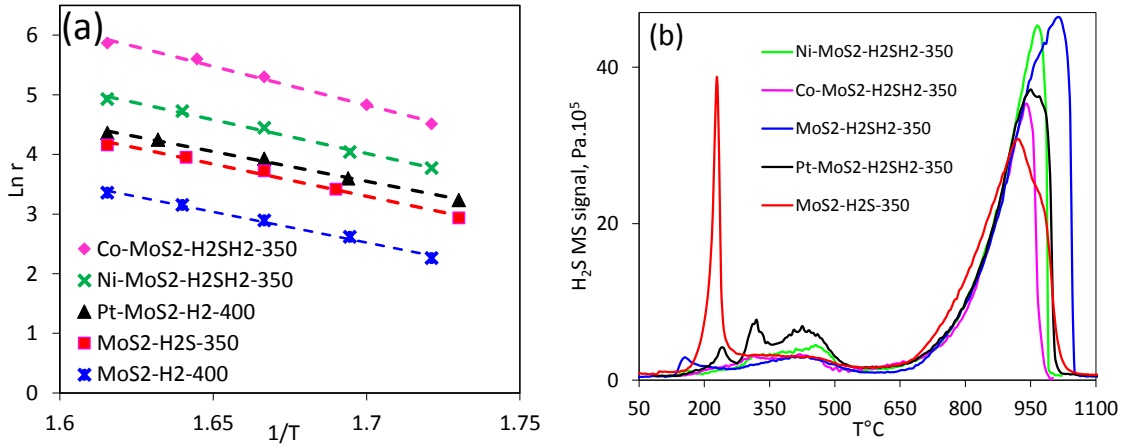

Fig. 1 (a) Arrhenius plots of thiophene HDS specific rate for the catalysts under study (b) TPR curves of H_2S release vs. temperature.

3.2. Thiophene HDS

The results of thiophene HDS test show strong variations of activity vs. the nature of the second transition metal, in the sequence Co > Ni > Pt. The highest degree of promotion was observed for cobalt: nearly fourfold increase of activity has been achieved vs. the non-promoted MoS_2-H_2S-350 sample (Fig. 1a). Similar promotion procedure carried out with nickel acetylacetonate resulted in a lower activity. We therefore expect lesser decoration effect of Ni and lesser difference of other properties between the Ni promoted sample and the non-promoted one, than for the Co-promoted solid. Platinum demonstrated a strong effect on the reducibility, but showed the weakest synergy effect. Probably, Pt atoms are not located at the decoration positions at the MoS_2 slabs edges, but detailed study of this question remains beyond the scope of this work. A twofold difference of the HDS activity between two non-promoted MoS_2 samples is due to the presence in MoS_2-H_2S-350 of more abundant SH groups, possessing hydrogenating properties [21]. Overall, the HDS activity test used here rather as a characterization technique, attests high degree of promotion for the Co – doped sample and confirms the expected differences between the non-promoted samples with different degree of reduction.

3.3. TPR study

TPR allows accessing interaction of MoS_2 with hydrogen and speciation of sulfur. The TPR curves of MoS_2 often show a sharp low-temperature peak (150-250 °C) appearing due to reduction of the S_2^{2-} moieties [38]. Similar sharp first peak has been observed on sulfur -saturated MoS_2 and on the amorphous sulfur-rich sulfides [39], having presumably chain-like structure with abundant S_2^{2-} groups in the structure (Fig. 2 a-c). After the first peak follows an intermediate zone with less intense H_2S release, smeared between 300 and 600 °C. Finally, ascending TPR branch appears above 700 °C, due to quasi-equilibrium bulk reduction [37]. TPR of MoS_2 has been studied by first-principles theory [31, 32]. The narrow first peak has been attributed to the reductive transition from 100%S covered Mo-edges to 50%S covered Mo-edges (Fig. 2 e-f). While the first TPR peak is well identified experimentally and explained by theory, no TPR features of the S-edges had ever been identified. Whether the M- and S- edges are reduced at similar temperatures, or on the contrary, S-edges are too stable (and therefore featureless in TPR) is not clear.

TPR patterns for the samples under study are shown in Fig 1b. For the solids prepared in hydrogen (MoS_2-H_2-400 and Pt-MoS_2-H_2-400), the TPR curves are obviously featureless below 400 °C and therefore not presented. Instead, TPR curves for the non-promoted MoS_2 and Pt-doped solid re-activated in 15% H_2S/H_2 mixture at 350 °C are given, to demonstrate change reducibility due to Pt addition (though these samples were not retained for the INS study and other experiments).

Sharp low-temperature TPR peak is expectedly present for MoS_2-H_2S-350. Its intensity is strongly decreased in the MoS_2-H_2SH_2-350 and both Co and Ni-promoted solids prepared under the same conditions. This finding agrees with the previous attribution of the first TPR peak to the reduction of 100% S-covered M edges. While the intensity of the first peak varies drastically, the broad reduction zone between 300 and 600 °C is invariably present and has similar shape for all preparations except Pt-containing one. According to phase diagrams [34], MoS_2-H_2S-350 sample is supposed to expose almost exclusively M-edges, whereas MoS_2-H_2-400 should contain an important part of S-edges. However the TPR pattern of MoS_2-H_2-400 does not show any particular features attributable to S-edges.

The TPR curve for Pt-containing sample shows higher reducibility vs. the non- doped sample prepared under the same conditions. Several small peaks appear for Pt-MoS_2-H_2-400, not typical for the individual MoS_2. As the amount of Pt is low and reduction of platinum sulfide not prone to give intense TPR features, these novel peaks correspond probably to a more sharply revealed reduction steps between the MoS_2 edges states of different sulfur coverage, which becomes possible due high hydrogen-activating power of platinum.

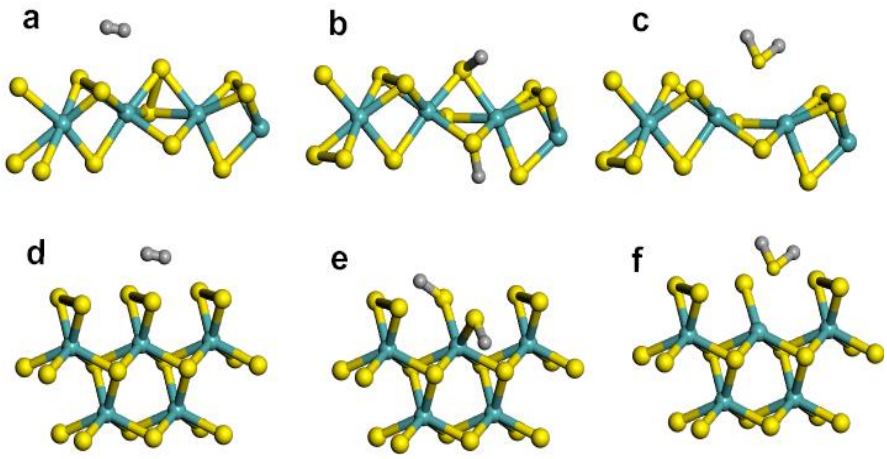

Fig. 2 Hypothetic TPR reaction pathways on amorphous MoS_3 (or sulfur-saturated S-edge) (a-c) and on sulfur saturated M-edge (d-f).

3.4. TPD of H_2 and H_2S.

Temperature programmed desorption experiments allowed quantifying the amount of hydrogen species in the solids by integration of TPD curves from room temperature to 1050 °C. Hydrogen species are released in two forms: as molecular H_2 (Fig. 2a) and as H_2S (Fig 2b). The amount of desorbed H_2 is comparable for all samples but it decreases in the sequence MoS_2-H_2S-350 > MoS_2-H_2-400 > Ni-MoS_2-H_2SH_2-350 > Pt-MoS_2-H_2-400. The overall amount of released H_2 decreases with the degree of sample reduction, but also it is lesser for the promoted solids than for the non-promoted ones. The H_2 TPD curves are shifted towards higher temperatures for more reduced samples. As with the desorbed H_2S, its amount strongly differs for the solids under study. For the MoS_2-H_2S-350 solid, almost one fifth of the total hydrogen is released as H_2S, whereas for Pt-MoS_2-H_2-400 and MoS_2-H_2-400 its amount is negligible, being lesser than 1% as compared

with the amount of desorbed H_2 (Table S3). As there is no physically adsorbed H_2S on the solids (vide infra), adsorbed hydrogen species is partially present as –SH groups for which thermal recombination leads to the release of H_2S.

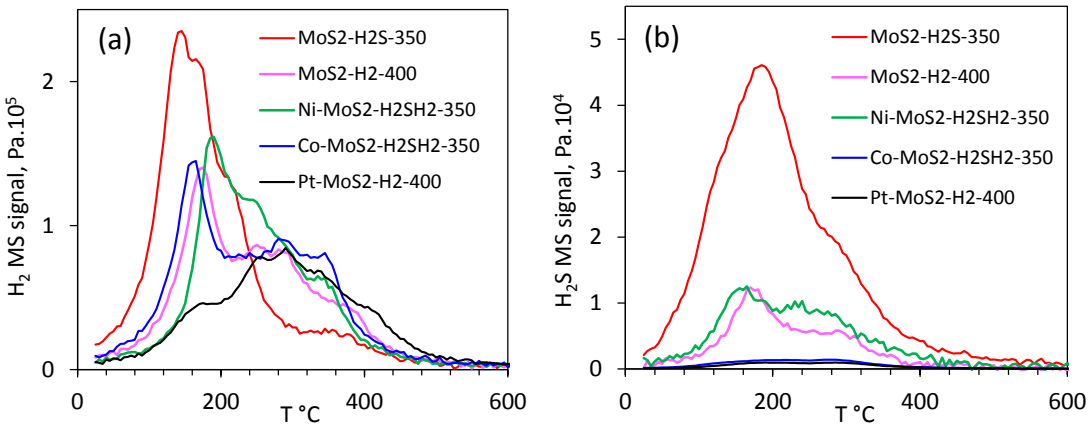

Fig. 3 TPD curves of H_2 (a) and H_2S (b) released from the solids under study upon heating in Ar flow.

Noteworthy, solution-synthesized amorphous sulfides such as oxysulfide CoSOH [40] and amorphous sulfur-rich sulfides MoS_x (x from 3 to 6) [39], when exposed to static hydrogen even at ambient conditions absorbed large amounts of hydrogen, (as high as 0.3 mol of H_2/Co atom and up to 0.5 mol H_2 / mol Mo) without any apparent changes in their structure. For these amorphous sulfides all sulfur atoms are involved in the S-S bridges and H_2 absorption occurs as formation of SH groups due to S-S bonds cleavage. Thermal desorption leads to release of hydrogen species mostly as H_2S. Therefore dominant form of desorbed H species strongly depends on the stoichiometry: higher is the excess of sulfur higher is the relative part released as H_2S.

3.5 INS experiment

Inelastic neutron scattering as a vibration spectroscopy has a great advantage for studying hydrogen in catalysts, because INS cross-section is much higher for hydrogen than for other elements [41]. Moreover it probes the whole Brilloin zone and has no selection rules, which makes attribution of the INS spectral lines quite straightforward. By contrast, as even for high-frequency modes the impacting neutrons are able to excite not only the first but several vibrational levels, the INS spectra usually show several

harmonic replicas of the same pattern. Beside the type of moving nuclei, INS cross section depends on the movement amplitude. That is why, inversely to IR- spectra, bending and wagging modes usually have higher INS amplitudes than stretching ones [42 43].

Heterolytic vs. homolytic H_2 adsorption on different sulfides has been studied by INS and actively debated in the literature. Thus, for H_2 adsorption on the ruthenium sulfide RuS_2, INS suggested heterolytic dissociative adsorption of H_2 with formation of Ru-H and S-H bonds [44] but in another study only SH groups were observed [45]. On the other hand, only SH groups were detected on amorphous MoS_x sulfides [39]. Therefore it was not a priori clear whether the M-H species could be present in the bimetallic catalysts or in the reduced MoS_2.

The INS spectra are shown in Fig. 4. The intensity of signal varies significantly, but the position of main peaks and their relative intensity is similar for all five materials. The maxima of all lines coincide within 10 cm^{-1} accuracy (Fig. S5). Therefore no change in the nature of main H species could be inferred whatever the sample and whatever the treatment temperature. For two differently treated samples of MoS_2 and three bimetallic materials, the major hydrogen species showed the vibration band at 83-85 meV (685-692 cm^{-1}) and its harmonics. Similar frequency was previously attributed to bending vibrations in the surface -S-H groups [15-20]. Due to anharmonicity effects [46] the frequencies of overtones are slightly lower than integer multiples of the main line (Fig. 4). The S-H stretching region at ca. 2500 cm^{-1} overlaps with the third harmonics of bending vibration and could not be analyzed. No evidence of Mo-H bonding, neither of M-H where M is a promoting atom (expected above 800 cm^{-1}) could be inferred from the INS spectra.

A pronounced shoulder is observed for the Co-promoted sample and for the MoS_2-H_2S-350 material in the range between 610 and 625 cm^{-1}. INS peaks decomposition with PEAKFIT software (Figure S6, Table S4) indicates that this shoulder peak is also present in other samples, but in much lesser amounts. Being relatively close to the main peak, this shoulder is probably also attributable to the S-H bending, but in a modified coordination.

The materials at stake are supposed to have different proportions of S- and M- edges, as well as (for promoted catalysts) considerable amounts of promoting atoms in the decoration position. The observed similarity of the main INS frequency could formally be explained in several ways. Either the stable H species have similar environment (and therefore vibration frequency) on both M- and S- edges, as well as on the promoted sites, or only one of two edges accommodates stable adsorbed H species. Another possible explanation is that only one type of edge structures is actually exposed in all samples. These alternatives are discussed in more detail in the next section.

The integral intensity of INS vibrations for five samples at stake correlates with the variations of the amount of hydrogen in the material, as determined from TPD experiments (Figure S7). The linear regression line has a slope close to 1 and crosses the Y axis near the origin. Therefore all the H species are probed by INS, and, other way around, no H species escape detection by TPD. Our values are close to reported by Polz et al [47], who studied the volumetric H_2 uptake on similar polycrystalline MoS_2 (39 m^2/g) and concluded that H_2 activation goes via homolytic dissociation.

Hydrogen uptake (Table 1) was always significantly lower than could be potentially accommodated by the edges at a hypothetic 1:1 Mo to H stoichiometry. Indeed, full edges coverage by H atoms would correspond to the stoichiometry in the range from $H_{0.31}MoS_{2+\delta}$ for 5 nm triangles to $H_{0.18}MoS_{2+\delta}$ for 6 nm hexagons (Fig. S8). The measured H_2 uptake values are several times lower than these theory values. The BET specific surface areas of all samples (51-64 m^2/g) are by order of magnitude lower than the theory values for single sheets. Indeed, theory surface area for monolayer fringes is higher than 550 m^2/g (for an infinite single sheet) and depends on the edges contribution (Fig. S9). Thus, edges surface for the 5-nm size triangular particles is 120 m^2/g, which is twice higher than the total measured BET surface areas. It means that the samples expose to nitrogen only a minor part of all edges. Stacking of slabs and agglomeration of stacks bundles are obvious reasons for this difference. It seems not clear however, what is the physical nature of the relationship between the total amount of edges available, the BET surface areas and the hydrogen uptake. Two alternative (non-mutually excluding) pictures are possible, which for better visual representation are sketched in Fig. S10.

In the first case (Fig. S10a) hydrogen is adsorbed only on the surface available for the BET measurements. As hydrogen is chemically adsorbed only on the edges and not on basal planes, the possible H_2 uptake corresponds to the part of edges in the total BET surface area. Under this assumption hydrogen H_2 should occur on approximately 10 % of total amount of slabs edges present in the solid. Then to explain the observed H_2 uptake, an edge H:Mo adsorption stoichiometry close to 2 should be assumed (Table S5). In the second hypothetic case, after being dissociated, atomic hydrogen can freely penetrate in between the agglomerates of stacks. Then, incomplete coverage of edges by H atoms (low H:Mo stoichiometry) should be assumed to explain the observed H_2 uptake.

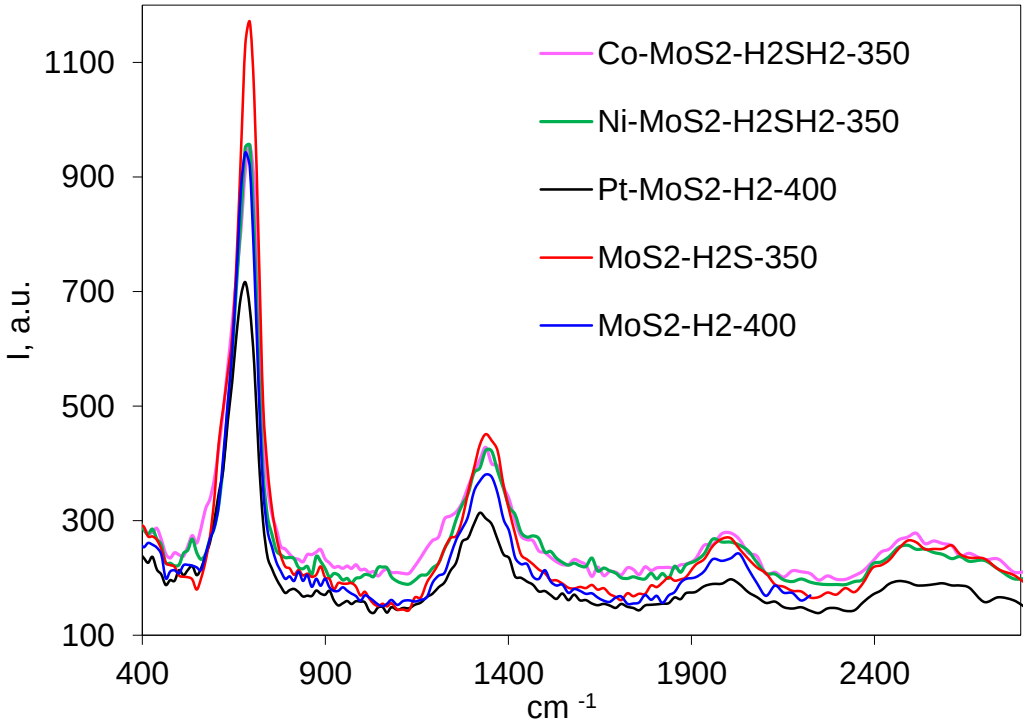

Fig. 4 INS spectra of the promoted and non-promoted Mo sulfides, treated with H_2 or H_2S.

At this point we cannot unravel these two effects, but the second hypothesis of uncomplete coverage seems more probable. Indeed, the edge H:Mo stoichiometry of 2 or higher seems chemically unreasonable, in particular for the samples treated at 400 °C, because it supposes existence of two thermally stable germinal SH groups at each edge Mo atom. Moreover, the observed H_2 uptake is not proportional to the BET surface area, as it should be in the first case. Thus, for two solids reduced at 400 °C, BET specific

surface areas and XRD/TEM morphologies are similar. However, one sample ($H_{0.044}MoS_{2.03}$) adsorbs considerably more hydrogen than another ($H_{0.024}PtMoS_{1.99}$). This difference could be explained only by different chemical properties of the edges.

3.6. Results of DFT calculations as compared with the INS spectra.

DFT calculations have been carried out to compare calculated and experimental frequencies and to explain the nature of observed low-frequency shoulder. Non-periodic calculations using ORCA code were carried out. However our results could be approximately compared with the previous plane-wave periodic calculations, where the M- and S- edges supercells of size comparable to our clusters were. As far as comparison is possible, our results are not far from those reported in the most recent calculations by Prodhomme et al. [32] using VASP code and PW91 functional. In our calculations we did not compare the energies, but focused on the frequency calculations for triangular clusters with S- and M-edge structures, similar to those reported previously [35]. In addition we study Co- substituted and corner configurations that seem plausible in such catalysts. As only cobalt showed high promotion effect and a significant difference of INS spectrum vs. non-promoted samples, Pt- and Ni- doped edges were not considered. On the other hand, since a compelling evidence exists of the co-existence of large amounts of S_2^{2-} and SH species in the MoS_2-H_2S-350 sample, we considered M- edges containing such moieties.

Significant relaxation from the ideal MoS_2 structure has been observed in all cases. Thus, in the 100% S-covered S-edge triangles, dimerization of the S as well as Mo-Mo bonds was observed as reported in [35]. Detailed analysis of these effects is beyond the scope of this study. The values of calculated vibrations frequencies are summarized in Table 2. A full list of the structures and the numeric conditions is given in Table S1.

Our calculations reproduce the experimental frequency of H_2S bending within 10 cm^{-1} range (exact value obtained for PBE0, Table S6). However for the Mo-containing clusters there are no benchmark experimental references and the error could be larger. As the published scaling factors for these functionals and basises vary from approximately 0.98 to 1.04 [48, 49], the overall accuracy of 20 cm^{-1} at the main line frequency 680-690 cm^{-1}

seems reasonable, i.e. the frequencies within the range 20 cm^{-1} around the experimental values could be considered as matching.

Several model structures give the SH bending vibration frequencies close enough to the experimental one (Table 2). These include Mo-SH-Mo bond on the 50 % and 100 % S covered S edge- like structures (entries 1 and 3), and to the 100% sulfur–covered M-edge configurations with germinal and vicinal SH groups (entries 9-11). As several configurations give an approximate match between the calculated and experimental frequencies, a simple selection of calculated frequency the closest to the experimental value is not sufficient to conclude on the nature of species. Chemical rationale is necessary to rule out certain species as main contributors and to privilege others.

An important caveat should be noted concerning the relative and the absolute accuracy of the DFT-calculated frequencies. It is well known that the relative values of vibration frequencies are much better predicted than the absolute values, so that additional scaling of frequencies is usually necessary [49]. Our DFT frequency calculation accuracy is about 20 cm^{-1}. Then if, for example DFT frequencies calculated for two alternative species A and B differ from the experimental value by 15 cm^{-1} and -15 cm^{-1}, then both A and B structures are matching as *absolute* values and we cannot decide from DFT only, which one of two is appropriate. However if both A and B structures were observed in a series of measurements, then DFT calculation would reliably predict the *relative* 30 cm^{-1} shift between them.

From the comparison between the observed and calculated frequencies, the presence of any significant amounts of physically adsorbed H_2S (1183 cm^{-1}) can be ruled out. By the same token, no stable Mo-H or Co-H species could be present in these systems (frequencies above 800 cm^{-1} , Table S6)

Isolated Mo-SH groups at the corner position (Table 2, entry 5) should give significantly lower bending frequency than experimentally observed and could be ruled out as well. By contrast, bridging Mo-SH-Mo groups at the 50% or 100% sulfur-covered S-edges (662 and 686 cm^{-1}, entries 1 and 3) are formally eligible as the main SH species. However, the (presumably all – M-edge) MoS_2-H_2S-350 solid shows the same frequency as in MoS_2-H_2-400 and Pt-MoS_2-H_2-400, potentially containing S-edges. As with 100 % S-covered S edges, they are not supposed to be formed neither in the MoS_2-H_2S-350 (because of 2D

morphology) nor in the MoS_2-H_2-400 and Pt—MoS_2-H_2-400 (because of edges reduction). The 50% S-edge could in principle be present in the MoS_2-H_2-400 and Pt-MoS_2-H_2-400 samples. However the frequency 662 cm^{-1} for 50% covered S-edge is sufficiently different from the frequencies expected for sulfur -saturated M edges (689, 697, 675 cm^{-1} respectively) to be detected as a systematic shift between sulfur-saturated and reduced samples, which is not the case. Therefore, hydrogen species located at the S-edges are not predominant in our samples. At best they are present simultaneously with the M-edge SH groups but are hidden due to the frequency overlap.

Previous DFT calculations [32] predict stretching modes at 1374 and 1285 cm^{-1} for 25 % covered S edge, due to bridging SH and MoH groups bonded in parallel to adjacent edge-Mo atoms. If present, these modes should overlap with the second harmonic of the main line having maximum at 1340-1350 cm^{-1}. However both the intensity and position of this second line follow the first one as the second harmonic should do, without anomalies. Such in-step behavior of the second line vs the main one leaves no much room for the eventual contribution of other species.

At the M-edge, several configurations have been considered, differing by approximate S coverage from 100 % to 25 %. Such configurations may contain μ_2 (bridging) and μ_1 (dangling) SH groups as well as S_2^{2-} surface moieties. Bridging Mo-SH-Mo groups are always formed after geometry optimization on the reduced surfaces (50% S coverage and below), whatever the initial configuration. For the bridging SH groups located at the reduced M –edges calculations give systematically lower frequencies than for the isolated dangling SH groups (Table 2, entries 6, 7 vs 9-11). As is well-known from the IR spectroscopy of oxides, the OH vibrations frequency varies in the sequence isolated > bridged > tri-bridged [50]. The magnitude of the effect in oxides vs. sulfides must be different, but chemical rationale is the same.

Our calculations suggest that if the predominant type of H species were changed from dangling to bridging SH bonds, then a tangible frequency decrease should be observed. No frequency decrease was observed experimentally for the reduced solids vs. sulfur-saturated ones. Therefore the presence of bridging SH groups on the M-edges as major species seems less probable.

Between the 100% and 50% sulfur coverage, multiple configurations could be proposed, in which isolated SH groups and disulfide moieties are present at the M-edge. Characterizations give evidence that in the sulfur-saturated sample abundant S_2^{2-} moieties are present simultaneously with the –SH groups (cf. TPR, TPD curves and XPS spectra). However, for the reduced samples, disulfide groups are virtually absent, but still the same SH species are detected in comparable amounts. Therefore the SH groups of the same type are present on the sulfur –saturated M edges (where they co-exist with the S_2^{2-} groups) and then on the reduced solids. We conclude then that the main SH bending INS signal belongs rather to the isolated SH groups in which Mo preserves six-coordinated state, as depicted in Table 2, entry 11. Such groups coexisting with the S_2^{2-} ones may be natural primary products of the interaction of sulfur –saturated slab with H_2, (Fig 2) but as we see from the INS experiment, they are formed already during preparation in pure H_2S, i.e. no formation of the hydrogen-less totally sulfur-covered edge (structure Fig 2d) is necessary. During the reduction with H_2, disulfide groups are eliminated. When sulfur coverage decreases below 50 %, the Mo-S-Mo bridges are formed, which are less reactive towards hydrogen, in step with the decrease of hydrogen uptake observed experimentally (remarkably, according to TPD, hydrogen uptake decreased by orders of magnitude for the MoS_2 reduced at 700 °C [21]).

The presence of abundant disulfide groups distinguishes sulfur saturated sample from others, and it correlated with appearance of a strong shoulder at 610-625 cm^{-1}. As show DFT calculations, appearance of a low-frequency signal could be explained by interaction between the disulfide and SH groups. Thus, if a single SH group is located between two S_2^{2-} moieties, then after geometry optimization it invariably turns toward one of them and interacts strongly. Geometry optimization leads to hydrogen bonded S-H-S species and the corresponding frequencies below the main experimental value, but closer to the position of shoulder (Table 2, entry 8). Again, an analogy seems relevant to the well-known effects in the IR-spectra of oxides, where hydrogen – bonded OH groups are broadened and have lower frequencies vs. isolated groups of the same chemical nature [45]. More generally, without considering a direct S-H-S bonding, the neighboring S_2^{2-} groups vibrations may interact with the SH- bending vibrations and modify (decrease) their frequencies. Group vibrations of S-S at 530-550 cm-1 and SH bending modes at

675-690 cm^{-1} are coupled and generate novel normal modes with the frequencies in between the values for the corresponding isolated groups. This effect may contribute to the appearance of a low-frequency shoulder.

For vicinal and geminal $(SH)_2$ species the calculated frequencies split into asymmetric and symmetric modes separated by ca. 10-20 cm^{-1} (entries 9-11 of Table 2). These modes should not be distinguishable as separate peaks by INS with its resolution of 20 cm^{-1}, but might contribute to line broadening. The presence of vicinal SH groups cannot be formally excluded yet seems less probable. Such structures should rather correspond to the transient states of irreversible reaction between H_2 and disulfide groups.

Cobalt-promoted sample showed the strongest low-frequency shoulder that distinguishes it from other bimetallic samples. Therefore Co-substituted structures have been studied to explain the origin of this pronounced feature at 610-625 cm^{-1}. If a Mo-SH fragment was substituted by a Co-SH one within the same structure, the resulting frequency was always significantly higher than in the corresponding all-Mo structure (entries 1, 2 and 4, 5). Therefore substitution of Mo by Co within the same structure is ruled out. On the other hand, if Co atom was put in a position adjacent to the Mo-SH group and coordination number of Co was lowered from 6 to 4, then we obtained a decreased SH frequency, matching the shoulder position (entry 14). Lowering of frequency was in this case due to transition from all –Mo structure with dangling SH bonds (entry 12) to the substituted structure with a bridging Co-SH-Mo fragment (entry 14). The bending frequency in such bridging SH group is higher than for the analogous Mo-SH-Mo structure, but lower than in the parent all-Mo structure with dangling SH bonds. It seems important that Mo atom linked to the SH group should remain six-coordinated, in order for the Mo-SH bond to be easily inclined towards the adjacent cobalt atom, to form a bridge (non-bonding S-Co distance of 2.4-2.5 Å). Otherwise, if the Mo atom is pentacoordinated, a dangling SH bond remains vertically oriented, formation of a bridge seems unfavorable and high frequency is predicted (entry 13).

Alternative explanation of the low-frequency shoulder in Co- promoted catalyst is formation of a “corner-like” structure (Table 2, entry 5). Such structure is naturally formed at the slabs corners, but also if Co atoms were grafted on top of the existing edges. These two possibilities (entries 14 and 5) cannot be unraveled on the basis of our

results. The final answer might be given only if coordination of cobalt within the promoted catalyst prepared using acetylacetonate method [33] would be established more accurately. Grafting of Co on-top of MoS_2 edges with creation of corner-like geometries seems plausible. Thus, XAS data for CoMoS catalysts show the coordination numbers of Co lower than they should be in the linear-edge substituted structures [51, 52].

Table 2 DFT calculated vibration frequencies for the triangular sulfide clusters (15 metal atoms, BP86 functional, TVZP basis and tight convergence).

No.	Edge	M-SH	S-H def.	S-S str.	S-H str.	Configuration
1	S, 50 %	Mo, Mo	662	-	2547	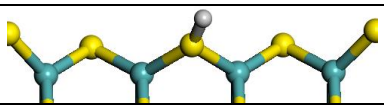
2	S, 50%	Co, Mo	686	-	2544	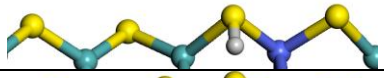
3	S, 100%	Mo, Mo	676	539	2555	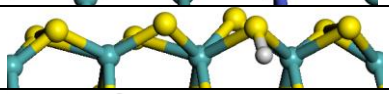
4	C	Co	618	-	2587	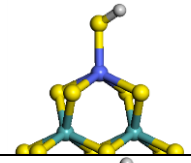
5	C	Mo, Mo	514	-	2593	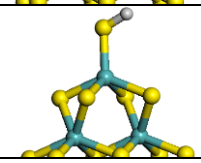
6	M, 25 %	Mo, Mo	557	-	2510	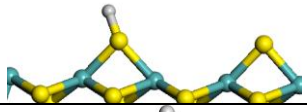
7	M 50%	Mo, Mo	618	-	2556	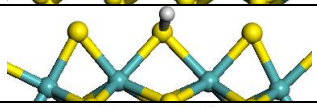
8	M 100 %	Mo, Mo	612	530	1850	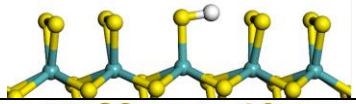
9	M 100 %	Mo	689a 662s	562	2569	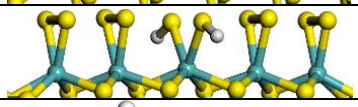
10	M 75 %	Mo (7)	697 668	523 554	2531 2542	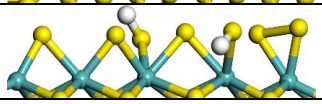
11	M 100%	Mo	675 664	536	2540 2550	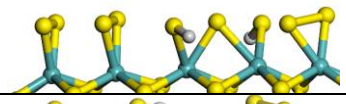
13	M 75 %	Mo	700	530	2570	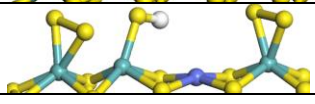

14	M 75%	Mo, Co	617	531	2555	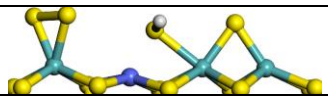
H_2S			1172		2627 2635	
H_2S exp [53,54]			1183		2616 2626	
MoS_2 Exp			**685-692** **610-625**			

Conclusions

The following conclusions can be drawn from the presented results:

(i) Only SH groups are formed as stable hydrogen-containing species on the surface of MoS_2-based solids under study (homolytic dissociation).

(ii) The same type of SH species is stable at the surface of nanocrystalline MoS_2, independently on the preparation conditions (H_2S, H_2 or H_2S/H_2 mixture) and on the presence of a second metal (Co, Ni, Pt). No tangible difference between the structures presumably exposing M- and S-edges could be identified.

(iii) The edges of sulfur-saturated MoS_2 prepared in pure H_2S, are not fully covered with S_2^{2-} species (as in Fig. 2d), but comparable amounts of SH and S_2^{2-} species coexist on them (as in Table 2, entry 11). Such configurations were neither previously demonstrated by experiment nor predicted by theory.

(iv) A low-frequency component (610-625 cm^{-1}) is systematically present in the INS spectra of our samples. This component is particularly intense for sulfur-saturated and for Co-promoted solids. It is attributable to the interaction between SH groups and S_2^{2-} species and/or adjacent Co atoms.

(v) Hydrogen uptake is higher than could be expected from the BET surface areas, suggesting that hydrogen penetrates between the stacks agglomerates to the edges inside the sample, unavailable for nitrogen adsorption.

(vi) Hydrogen uptake decreases with the degree of reduction of MoS_2 edges. However, complete elimination of observable S_2^{2-} moieties from the surface by reduction at 400 °C leads only to a moderate decrease of the amount of hydrogen species.

Stability and abundance of SH groups on the edges of MoS_2 slabs as demonstrated here, obviously impacts the models applied and the interpretations given to other characterizations, such as, for example, low-temperature CO adsorption [55, 56]. Indeed,

even if the presence of surface hydrogen species at the HDS reaction temperatures had been debated [25, 31], the SH groups are massively present at the temperatures of characterization experiments (ambient, 100 K). Preliminary DFT results show that the presence of SH groups might strongly impact the frequencies of adsorbed CO.

Beyond MoS_2, many studies have been focused on the interaction of H_2 with other lamellar sulfides. Some of them, such as NbS_2 and TaS_2 can intercalate hydrogen within the layers, whereas others, such as WS_2 [57] do not intercalate but adsorb hydrogen on the surface. Interaction of sulfides with hydrogen has both fundamental and practical interest not only for heterogeneous catalysis and not only for molybdenum, but for other metals and for other applications, such as electrocatalysts [58] or sensors [59].

ACKNOWLEDGEMENT
We thank Aleksander Ivanov for technical assistance at ILL

References

[1] Topsøe, H. The Role of Co–Mo–S Type Structures in Hydrotreating Catalysts. Appl. Catal. A: Gen. 322 (2007) 3– 8.
[2] S. Eijsbouts, S.W. Mayo, K. Fujita, Unsupported transition metal sulfide catalysts: From fundamentals to industrial application, App. Catal. A: Gen. 322 (2007) 58–66.
[3] J.N. Díaz de León, C. Ramesh Kumar, J. Antúnez-García, S. Fuentes-Moyado, Recent Insights in Transition Metal Sulfide Hydrodesulfurization Catalysts for the Production of Ultra Low Sulfur Diesel: A Short Review, Catalysts. 9 (2019) 87.
[4] Y. Zhang, J. Monnier, M. Ikura, Bio-oil upgrading using dispersed unsupported MoS_2 catalyst, Fuel Proc. Tech. 206 (2020) 106403.
[5] K.J. Smith, R.G. Herman, K. Klier, Kinetic modelling of higher alcohol synthesis over alkali-promoted Cu/ZnO and MoS2 catalysts, Chem. Eng. Sci. 45 (1990) 2639–2646.
[6] N. Wang, J. Li, R. Hu, Y. Zhang, H. Su, X. Gu, Enhanced catalytic performance and promotional effect of molybdenum sulfide cluster-derived catalysts for higher alcohols synthesis from syngas, Catal. Today. 316 (2018) 177–184.
[7] B.K. Miremadi, S.R. Morrison, High activity catalyst from exfoliated MoS_2, J. Catal. 103 (1987) 334–345.
[8] A. Primo, J. He, B. Jurca, B. Cojocaru, C. Bucur, V.I. Parvulescu, H. Garcia, CO_2 methanation catalyzed by oriented MoS_2 nanoplatelets supported on few layers graphene, Appl. Catal. B: Env. 245 (2019) 351–359.
[9] S. Yun, V. Guliants, Size-dependent catalytic behavior of MoS_2 nanoparticles in water-gas shift reaction, Catal. Comm. 140 (2020) 105990.
[10] J.D. Benck, T.R. Hellstern, J. Kibsgaard, P. Chakthranont, T.F. Jaramillo, Catalyzing the Hydrogen Evolution Reaction (HER) with Molybdenum Sulfide Nanomaterials, ACS Catal. 4 (2014) 3957–3971.
[11] A. Tahira, Z.H. Ibupoto, R. Mazzaro, S. You, V. Morandi, M.M. Natile, M. Vagin, A. Vomiero, Advanced Electrocatalysts for Hydrogen Evolution Reaction Based on Core–Shell MoS_2/TiO_2 Nanostructures in Acidic and Alkaline Media, ACS Appl. Energy Mater. 2 (2019) 2053–2062.

[12] P.C.K. Vesborg, B. Seger, I. Chorkendorff, Recent Development in Hydrogen Evolution Reaction Catalysts and Their Practical Implementation, J. Phys. Chem. Lett. 6 (2015) 951–957.
[13] A.B. Laursen, S. Kegnæs, S. Dahl, I. Chorkendorff, Molybdenum sulfides—efficient and viable materials for electro - and photoelectrocatalytic hydrogen evolution, Energy Environ. Sci. 5 (2012) 5577–5591.
[14] N.Y. Topsoe, H. Topsoe, FTIR Studies of Mo/Al_2O_3-Based Catalysts: II. Evidence for the Presence of SH Groups and Their Role in Acidity and Activity, J. Catal. 139 (1993) 641–651. https://doi.org/10.1006/jcat.1993.1056.
[15] P.N. Jones, E. Knözinger, W. Langel, R.B. Moyes, J. Tomkinson, Adsorption of molecular hydrogen at high pressure and temperature on MoS2 and WS2; observed by inelastic neutron scattering, Surf. Sci. 207 (1988) 159–176.
[16] C.J. Wright, C. Sampson, D. Fraser, R.B. Moyes, P.B. Wells, C. Riekel, Hydrogen sorption by molybdenum sulphide catalysts, J. Chem. Soc., Faraday Trans. 1. 76 (1980) 1585–1598.
[17] S. Vasudevan, J.M. Thomas, C.J. Wright, C. Sampson, Inelastic neutron scattering studies of hydrogen uptake by a model hydrodesulphurization catalyst at high pressure, J. Chem. Soc., Chem. Commun. (1982) 418–419.
[18] C. Sampson, J.M. Thomas, S. Vasudevan, C.J. Wright, A preliminary investigation of the sorption of hydrogen at high pressure by MoS_2, Bull. Soc. Chim. Belg. 90 (1981) 1215–1224.
[19] P. Sundberg, R.B. Moyes, J. Tomkinson, Inelastic Neutron Scattering Spectroscopy of Hydrogen Adsorbed on Powdered-MoS_2, MoS_2-Alumina and Nickel-Promoted MoS_2, Bull. Soc. Chim. Belg. 100 (1991) 967–976.
[20] P.C.H. Mitchell, D.A. Green, E. Payen, A.C. Evans, Hydrogen in molybdenum and cobalt sulfide catalysts. A neutron Compton scattering study on the ISIS electronvolt spectrometer, J. Chem. Soc., Faraday Trans. 91 (1995) 4467–4469.
[21] P. Afanasiev, The influence of reducing and sulfiding conditions on the properties of unsupported MoS_2-based catalysts, J. Catal. 269 (2010) 269–280.
[22] P. Raybaud, H. Toulhoat, Catalysis by Transition Metal Sulphides: From Molecular Theory to Industrial Application, Editions TECHNIP, 2013.
[23] M. Breysse, E. Furimsky, S. Kasztelan, M. Lacroix, G. Perot, Hydrogen Activation by Transition Metal Sulfides, Catal. Rev. 44 (2002) 651–735.
[24] L.S. Byskov, M. Bollinger, J.K. Nørskov, B.S. Clausen, H. Topsøe, Molecular aspects of the H_2 activation on MoS_2 based catalysts — the role of dynamic surface arrangements, J. Molec. Catal. A: Chem. 163 (2000) 117–122.
[25] L.S. Byskov, J.K. Nørskov, B.S. Clausen, H. Topsøe, DFT Calculations of Unpromoted and Promoted MoS_2-Based Hydrodesulfurization Catalysts, J. Catal. 187 (1999) 109–122.
[26] S. Cristol, J.F. Paul, E. Payen, D. Bougeard, S. Clémendot, F. Hutschka, Theoretical Study of the MoS_2 (100) Surface: A Chemical Potential Analysis of Sulfur and Hydrogen Coverage. 2. Effect of the Total Pressure on Surface Stability, J. Phys. Chem. B. 106 (2002) 5659–5667.
[27] A. Travert, H. Nakamura, R.A. van Santen, S. Cristol, J.-F. Paul, E. Payen, Hydrogen Activation on Mo-Based Sulfide Catalysts, a Periodic DFT Study, J. Am. Chem. Soc. 124 (2002) 7084–7095.
[28] M. Sun, A.E. Nelson, J. Adjaye, Ab initio DFT study of hydrogen dissociation on MoS_2, NiMoS, and CoMoS: mechanism, kinetics, and vibrational frequencies, J. Catal. 233 (2005) 411–421.
[29] M. Sun, A.E. Nelson, J. Adjaye, Adsorption and dissociation of H_2 and H_2S on MoS_2 and NiMoS catalysts, Catalysis Today. 105 (2005) 36–43.
[30] J.V. Lauritsen, M.V. Bollinger, E. Lægsgaard, K.W. Jacobsen, J.K. Nørskov, B.S. Clausen, H. Topsøe, F. Besenbacher, Atomic-scale insight into structure and morphology changes of MoS_2 nanoclusters in hydrotreating catalysts, J. Catal. 221 (2004) 510–522.

[31] N. Dinter, M. Rusanen, P. Raybaud, S. Kasztelan, P. da Silva, H. Toulhoat, Temperature-programed reduction of unpromoted MoS_2-based hydrodesulfurization catalysts: Experiments and kinetic modeling from first principles, J. Catal. 267 (2009) 67–77.
[32] P.-Y. Prodhomme, P. Raybaud, H. Toulhoat, Free-energy profiles along reduction pathways of MoS_2 M-edge and S-edge by dihydrogen: A first-principles study, J. Catal. 280 (2011) 178–195.
[33] I. Bezverkhyy, P. Afanasiev, M. Lacroix, Promotion of highly loaded MoS_2/Al_2O_3 hydrodesulfurization catalysts prepared in aqueous solution, J. Catal. 230 (2005) 133–139.
[34] F. Neese, The ORCA program system. Wiley interdisciplinary Reviews - Computational Molecular Science, 2 (2012) 73–78.
[35] H. Schweiger, P. Raybaud, G. Kresse, H. Toulhoat, Shape and Edge Sites Modifications of MoS_2 Catalytic Nanoparticles Induced by Working Conditions: A Theoretical Study, J. Catal. 207 (2002) 76–87.
[36] P. Afanasiev, C. Lorentz, Oxidation of Nanodispersed MoS_2 in Ambient Air: The Products and the Mechanistic Steps, J. Phys. Chem. C. 123 (2019) 7486–7494.
[37] V. Costa, B. Guichard, M. Digne, C. Legens, P. Lecour, K. Marchand, P. Raybaud, E. Krebs, C. Geantet, A rational interpretation of improved catalytic performances of additive-impregnated dried CoMo hydrotreating catalysts: A combined theoretical and experimental study, Catal. Sci. Technol. 3 (2012) 140–151.
[38] P. Afanasiev, On the interpretation of temperature programmed reduction patterns of transition metals sulphides, Appl. Catal. A-Gen. 303 (2006) 110–115.
[39] P. Afanasiev, H. Jobic, C. Lorentz, P. Leverd, N. Mastubayashi, L. Piccolo, M. Vrinat, Low-Temperature Hydrogen Interaction with Amorphous Molybdenum Sulfides MoS_x, J. Phys. Chem. C. 113 (2009) 4139–4146.
[40] C. Loussot, P. Afanasiev, M. Vrinat, H. Jobic, P.C. Leverd, Amorphous Cobalt Oxysulfide as a Hydrogen Trap, Chem. Mater. 18 (2006) 5659–5668.
[41] P.W. Albers, S.F. Parker, Inelastic Incoherent Neutron Scattering in Catalysis Research, in: B.C. Gates, H. Knözinger (Eds.), Advances in Catalysis, Academic Press, 2007: pp. 99–132.
[42] B.S. Hudson, Chapter 17 - Vibrational Spectroscopy via Inelastic Neutron Scattering, in: J. Laane (Ed.), Frontiers of Molecular Spectroscopy, Elsevier, Amsterdam, 2009: pp. 597–622.
[43] B.S. Hudson, Inelastic Neutron Scattering: A Tool in Molecular Vibrational Spectroscopy and a Test of ab Initio Methods, J. Phys. Chem. A. 105 (2001) 3949–3960.
[44] M. Lacroix, H. Jobic, C. Dumonteil, P. Afanasiev, M. Breysse, S. Kasztelan, Role of adsorbed hydrogen species on ruthenium and molybdenum sulfides. Characterization by inelastic neutron scattering, thermoanalysis methods and model reactions, Elsevier Science Publ B V, Amsterdam, 1996.
[45] W.H. Heise, K. Lu, Y.J. Kuo, T.J. Udovic, J.J. Rush, B.J. Tatarchuk, Neutron scattering study of hydrogen on ruthenium sulfide, J. Phys. Chem. 92 (1988) 5184–5188.
[46] C. Mungan, U. Happek, T. Hossain, A. Sievers, Infrared spectroscopy of the stretching modes of SeH− and TeH− in KCl and KBr, Journal of Physics and Chemistry of Solids. 56 (1995) 735–743.
[47] J. Polz, H. Zeilinger, B. Müller, H. Knözinger, Hydrogen uptake by MoS_2 and sulfided alumina-supported Mo catalysts, J. Catal. 120 (1989) 22-28.
[48] A.P. Scott, L. Radom, Harmonic Vibrational Frequencies: An Evaluation of Hartree−Fock, Møller−Plesset, Quadratic Configuration Interaction, Density Functional Theory, and Semiempirical Scale Factors, J. Phys. Chem. 100 (1996) 16502–16513.
[49] M.A. Palafox, DFT computations on vibrational spectra: Scaling procedures to improve the wavenumbers, Physical Sciences Reviews. 3 (2018).
[50] X. Liu, R.E. Truitt, DRFT-IR Studies of the Surface of γ-Alumina, J. Am. Chem. Soc. 119 (1997) 9856–9860.

[51] B.R.G. Leliveld, J.A.J. van Dillen, J.W. Geus, D.C. Koningsberger, M. de Boer, Structure and Nature of the Active Sites in CoMo Hydrotreating Catalysts. An EXAFS Study of the Reaction with Selenophene, J. Phys. Chem. B. 101 (1997) 11160–11171.
[52] L. Plais, C. Lancelot, C. Lamonier, E. Payen, V. Briois, First in situ temperature quantification of CoMoS species upon gas sulfidation enabled by new insight on cobalt sulfide formation, Catal. Today. In press (2020).
[53] A.A.A. Azzam, J. Tennyson, S.N. Yurchenko, O.V. Naumenko, ExoMol molecular line lists – XVI. The rotation–vibration spectrum of hot H_2S, Mon Not R Astron Soc. 460 (2016) 4063–4074.
[54] W. C. Lane, T. H. Edwards, J. R. Gillis, F. S.Bonomo, F. J. Murcray Analysis of ν_2 of H_2S, Journal of Molecular Spectroscopy. 95 (1982) 365–380.
[55] A. Travert, C. Dujardin, F. Maugé, S. Cristol, J.F. Paul, E. Payen, D. Bougeard, Parallel between infrared characterisation and ab initio calculations of CO adsorption on sulphided Mo catalysts, Catal. Today. 70 (2001) 255–269.
[56] F. Cesano, S. Bertarione, A. Piovano, G. Agostini, M.M. Rahman, E. Groppo, F. Bonino, D. Scarano, C. Lamberti, S. Bordiga, L. Montanari, L. Bonoldi, R. Millini, A. Zecchina, Model oxide supported MoS_2 HDS catalysts: structure and surface properties, Catal. Sci. Technol. 1 (2011) 123–136.
[57] C.J. Wright, D. Fraser, R.B. Moyes, P.B. Wells, The adsorption of hydrogen and hydrogen sulphide on tungsten sulphide; isotherm and neutron scattering studies, Appl. Catal. 1 (1981) 49–58.
[58] J. Shi, X. Wang, S. Zhang, L. Xiao, Y. Huan, Y. Gong, Z. Zhang, Y. Li, X. Zhou, M. Hong, Q. Fang, Q. Zhang, X. Liu, L. Gu, Z. Liu, Y. Zhang, Two-dimensional metallic tantalum disulfide as a hydrogen evolution catalyst, Nature Communications. 8 (2017) 958.
[59] C.H. Park, W.-T. Koo, Y.J. Lee, Y.H. Kim, J. Lee, J.-S. Jang, H. Yun, I.-D. Kim, B.J. Kim, Hydrogen Sensors Based on MoS_2 Hollow Architectures Assembled by Pickering Emulsion, ACS Nano. 14 (2020) 9652–9661.

Graphical abstract